Journal of Hazardous Materials, 36 (1994) 19–33
Elsevier Science Publishers B.V., Amsterdam

Pyrolysis of refuse derived fuel: Kinetic modelling from product composition

M. Rovatti, A. Converti*, M. Bisi and G. Ferraiolo

Institute of Chemical Engineering Science and Technology, University of Genoa, Via Opera Pia 15, 16145, Genoa (Italy)

(Received May 22, 1992; accepted in revised form April 2, 1993)

Abstract

The pyrolysis of RDF has been studied in this work by analyzing the gaseous product composition at different temperatures and reaction times. The formation of each gaseous component in the pyrolysis gas has been described by supposing the occurrence of simultaneous first-order reactions as well as neglecting possible interactions among them. This kinetic approach allows the calculation of the rate constants of formation for each product at different temperatures and the related thermodynamic quantities and the formulation of hypotheses on the mechanisms involved in the pyrolysis. Concerted mechanisms are proposed for the formation of most of the detected gaseous products.

1. Introduction

The pyrolysis and gasification processes, widely applied up to now to the treatment of special refuses such as rubber, exhausted oils and plastics, can constitute a valid alternative to incineration of the fraction of municipal solid wastes (MSW) which can be utilized as a fuel, the so-called refuse derived fuel (RDF). In fact, according to Buekens and Schoeters [1], these processes allow recycling of valuable materials, to produce fuel products and to reduce, at the same time, the total volume of emissions.

Several papers have been reported in the literature on the kinetics and thermodynamics of pyrolysis of the cellulosic fraction of municipal solid wastes [2, 3] and biomass [4]. Thurner and Mann described the pyrolysis of wood, utilizing the so-called "Three Reaction Model" to describe the simultaneous production of gas, tar and char [5]. The same model was successfully used [2] with the experimental results of Lipska and Parker on the pyrolysis of cellulose [6]. Several atomic species appear to stimulate the formation of char

* Author to whom correspondence should be adressed. Fax (+39 10) 353-2586.

SSDI 0304-3894(93)E0048-7

at the expense of tar and gas, while others, like potassium ions, are good aids for steam gasification [7]. Furthermore, Scott and Piskorz studied the effects of catalysts or inhibitors and lime addition, particle size, and other reaction environments on the pyrolysis of cellulosic biomass [8]. Finally, a kinetic model has recently been proposed by Koufopanos et al. to describe pyrolysis reactions influenced by secondary reactions between gaseous products and carbonaceous products inside the biomass particles [9].

Only a few attempts have been made, on the other hand, to carry out systematic studies on RDF. This refuse contains (in Italy), in addition to the cellulosic fraction (64%), significant amounts of plastics (about 26%) and other materials (about 10%); thus the kinetics of its pyrolysis are strongly influenced by unavoidable variations in the composition of the refuse.

In this study the experimental data of RDF pyrolysis in the absence of a sweep gas are presented and discussed, assuming that secondary reactions do not play a significant role during this specific process.

The model proposed here to carry out a kinetic evaluation of these results is intentionally based on the formation of gases rather than on the consumption of the reactants because the pyrolysis products are always the same, whereas the refuse composition is extremely variable case by case.

In the final part of this study, the activation entropy as well as the other thermodynamic quantities have been calculated by means of a standard graphical procedure. Although not rigorous, this procedure allows us to get some rough hints on the reaction mechanisms involved in the pyrolytic process of this fraction.

2. Materials and methods

2.1. The experimental setup

The flowsheet of the experimental setup is shown in Fig. 1. The reactor consists of a 650 mm long cylindrical chamber with diameter of 35 mm, built up using AISI 310 steel and heated through a tubular electric furnace (B) [10]. The furnace has been constructed to heat the reaction chamber up to the selected temperature in a few minutes. One end of the reactor was stoppered by a threaded plug, whereas the other remained open to allow the produced gas free to flow into a 450 mm high glassy bubble condenser (C), where heat was exchanged by indirect contact with water at room temperature flowing upstream. The condenser was followed by a glass-wool filter (F) to retain the dust that eventually escaped from the tar formed during the pyrolysis or from the condensate.

The gas was then collected into several graduated gasometers (G) arranged in parallel in order to evaluate the emitted gas volume as well as to obtain samples for analysis.

The refuse employed as starting material in this work was produced in a MSW treatment plant for compost and RDF productions in northern Italy,

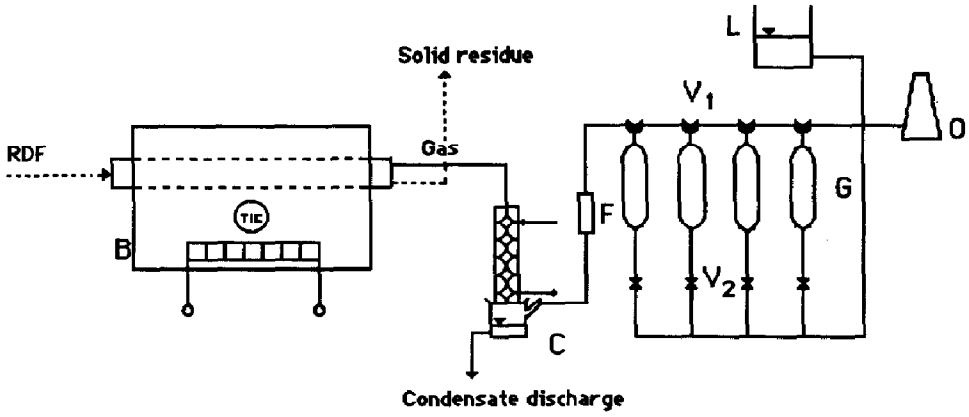

Fig. 1. Experimental setup: B tubular furnace, C condenser, F filter, G gasometers, L water reservoir, O stack, V1 three-way valves and V2 valves.

TABLE 1

Marketing and elemental composition of refuse derived fuel employed in this study

a. Marketing composition

Component	Percentage by weight (%)
Paper and cardboard	64
Plastics	26
Textile fibres	4
Natural fibres	6

b. Elemental composition

Element	Percentage by weight (%)
Carbon	44–48
Hydrogen	5.0–6.5
Oxygen	7–36
Nitrogen	0.6–0.7
Sulphur	0.2–0.3
Chlorine	0.10–0.18

destined to be used as a poor fuel in the cement industry. The average marketing composition of fluffy RDF is reported in Table 1a. Due to its heterogeneity, the elemental composition of RDF was very difficult to determine; hence, the material was always thoroughly crushed and homogenized to prepare samples for pyrolysis. For this reason ranges of compositions are reported in Table 1b for each element.

The fluffy RDF has been crushed in order to obtain particles with average size of 5 mm. In addition most of these particles are constituted by thin paper and plastics, so as to obtain nearly isothermal conditions, during the process of pyrolysis [11].

2.2. Operating conditions

Each test was carried out using 24 g of selected RDF samples and repeated until reliable series of data were obtained. Several samples of gaseous products were collected at time intervals of about 5 min (up to 1 h from the beginning of each test) and under different temperature conditions (namely 400, 500, 600, 700, 800 and 900 °C) and then analyzed according to the procedures described later. Liquid and solid products were sampled and analyzed only after each pyrolysis test was ended.

Due to heat-transfer limitations, the ratio between the heat-up time and the total time required to complete a run was always less than 0.1. This parameter was calculated during each run measuring the temperature in the bed of pyrolyzing RDF by means of a thermocouple.

The gas produced was analyzed for CH_4, CO_2, CO, H_2, and C_2H_4 by means of gas chromatography employing adequate detectors according to circumstances (thermoconductivity, flame ionization, mass spectrophotometry, etc.).

Hydrochloric acid content in the pyrolysis gas was analyzed by means of a colorimetric method [12].

Condensable products were extracted after each test from the bottom of the condenser and gravimetrically quantified. The liquid products were qualitatively analyzed with a gas chromatograph equipped with gas mass detector in order to evaluate the main organic compounds observed in the liquid. The amount of solid residue produced was determined by dry weight at the end of each run.

3. Experimental results

Figure 2 shows the results obtained at different temperatures in terms of produced volumes for each gaseous component ($V_{max,i}$); they refer to the maximum volume attainable for each gas at a given temperature by prolonging the pyrolysis until no further production was detected. Other gases, such as C_2H_6, NO_x, etc., have not been considered in this study because they were present in negligible amounts.

The changes of $V_i/V_{max,i}$ with T can be deduced by the curves of Fig. 3, with V_i evaluated at 60 min. For all gases, an increase in T brings about a corresponding increase of the conversion ratio as the obvious result of more favourable thermodynamic conditions.

The curves of Fig. 2 show that, above 700 °C, methane and carbon dioxide productions decrease with increasing temperature; on the other hand, hydrogen production increases continuously, whereas the maximum volume of CO

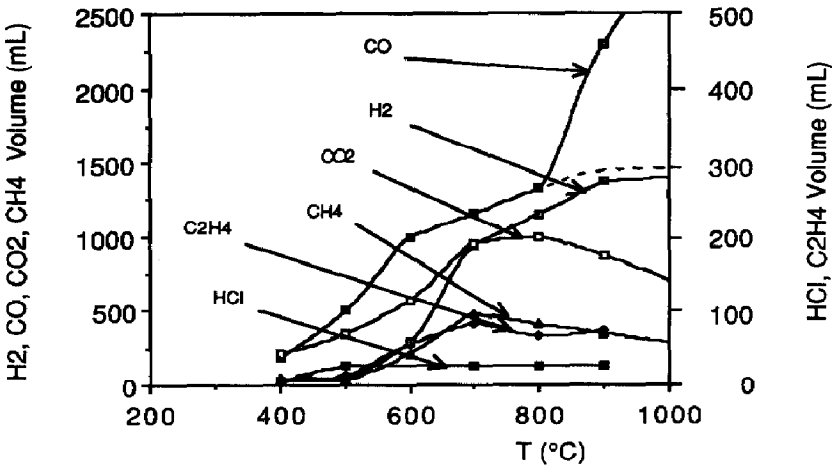

Fig. 2. Maximum gases production during pyrolysis of RDF at different temperatures. (- - -) expected trend; (——) experimental behaviour.

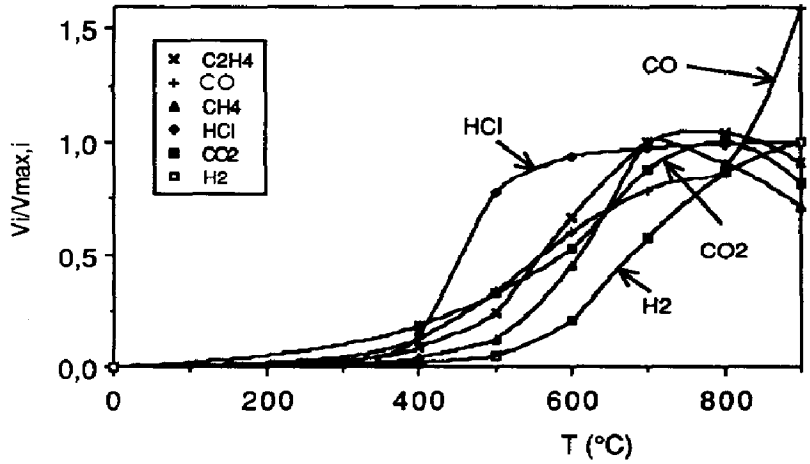

Fig. 3. Dependence of $V_i/V_{max,i}$ on temperature for each component of pyrolysis gas, with V_i calculated at 60 min.

produced at 900 °C is considerably higher than the value reasonably expectable from the trend of CO production up to 800 °C.

The simultaneous increase of CO and decrease of CO_2 with increasing the temperature above 700 °C could be explained with the occurrence of the well-known equilibrium of Boudouard:

$$C + CO_2 \rightleftharpoons 2\,CO$$

This reaction, if pure components are used, should proceed towards the formation of carbon dioxide below 600 °C, whereas CO formation becomes

predominant over 750 °C [13]. This secondary reaction can affect the calculation of both kinetic and thermodynamic constants at 900 °C.

For this reason, $V_{max,i}$ for CO has been extrapolated by means of the dashed curve of Fig. 2 for a hypothetical situation as though this secondary reaction were negligible.

As regards the methane behaviour up to 700 °C, it could be reasonably ascribed to the fact that the high molecular weight hydrocarbons constituting the RDF (mainly plastics, rubber, etc.) would be predominantly transformed, through rearrangement and/or transposition reactions, into hydrocarbons with low molecular weights. In practice, owing to the greater stability of CH_4 with respect to the other simple hydrocarbons, methane production is always favoured in the rupture of C–C bonds. As is well known, above 700 °C, on the contrary, the elemental components, C and H_2, become thermodynamically more stable than CH_4.

As regards the liquid products, highly polluted condensate rich in hydrochloric acid has been obtained instead of a fuel liquid phase, as reported for solid wastes [1], probably owing to the specific marketing composition of the RDF used in our tests. Among the main substances, identified through gas mass chromatography, i.e. acetone, 2-butanone, acetic acid, acetaldehyde, cyclohexanone, phenol, etc., one can notice the absence of organo-chlorinated pollutants, like PCB, PCDD and PCDF in the condensate, which means that all chlorine contained in the refuse is quantitatively converted into HCl. Furthermore, significant amounts of tar were detected, mainly in the pipes linking the reactor with the condenser.

The solid residues were formed as carbonaceous dusts with a heat value of about 18,000 kJ/kg. The total amount of ashes contained in the solid residue after pyrolysis ranged from 12% at 400 °C up to a maximum of 24% at 900 °C.

The material balances at the different temperatures tested are listed in Table 2. Water forms the major part of the liquid residues reported in this Table. These data point out that the amount of total gas produced at 900 °C is about eight times as high as at 400 °C, whereas both char and tar productions decrease markedly [10].

TABLE 2

Material balances for RDF pyrolysis at different temperatures

T (°C)	Solid residue (g)	Liquid residue (g)	Gas (g)	Tar (g)	Total (g)
400	14.35	5.30	0.63	3.72	24
500	13.95	5.90	1.53	2.72	24
600	12.00	6.50	2.71	2.79	24
700	9.15	8.00	4.20	2.65	24
800	8.90	8.60	4.10	2.40	24
900	8.00	9.29	5.55	1.16	24

4. Kinetic modelling

4.1. Model design

As demonstrated by Thurner and Mann for the pyrolysis of wood [5] and subsequently by Agrawal for that of cellulose [2], the simultaneous formations of three classes of products have been proved in this study also for RDF. According to their own volatility, the pyrolysis products can be subdivided in char, tar and gases.

The model employed in this study supposes that the pyrolytic degradation of RDF occurs homogeneously via three first-order competitive reactions:

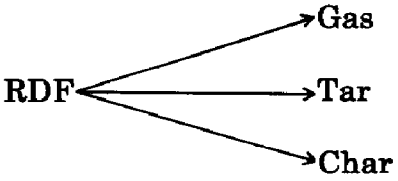

This work is aimed at setting up a suitable model describing the kinetics only of those reactions involved in the pyrolysis of RDF that lead to gas production. As far as the average composition of the gas fraction is concerned, a similar approach to the one proposed for the whole pyrolysis products has been followed, in that, as a first assumption, the pyrolysis of RDF would proceed via different parallel first-order competitive reactions and the gaseous products do not interact with each other.

According to the first-order reaction assumed, one can write for the production of each gas:

$$\ln c_i/c_{o,i} = -k_{o,i}\, t \tag{1}$$

where c_i is the residual concentration of the raw material after a time t, referring only to that fraction of the refuse actually convertible into the ith gaseous product, $k_{o,i}$ the respective specific rate constant, and $c_{o,i}$ the concentration of the starting material actually convertible into the ith product.

Since the refuse composition is extremely variable case by case, whilst the pyrolysis products are always the same, for simplicity the kinetic model has been intentionally based in this study on the development of gases rather than on the consumption of the reactants. To this purpose, c_i can be related to the concentration of each gaseous product (P_i) at a given reaction time according to the relation:

$$P_i = \alpha_i\,(c_{o,i} - c_i) \tag{2}$$

where α_i is a conversion yield depending on the type of gas.

Furthermore, $c_{o,i}$ can be related through the same conversion yield (α_i) to the maximum product threshold value ($P_{max,i}$):

$$P_{max,i} = \alpha_i c_{o,i} \tag{3}$$

By substituting eqs. (2) and (3) into eq. (1), we obtain

$$\ln[(P_{\max,i}-P_i)/P_{\max,i}] = -k_{o,i}t \tag{4}$$

Since the ratio of $(P_{\max,i}-P_i)$ to $P_{\max,i}$ is dimensionless, the volumes of produced gases have been directly used in eq. (4) instead of the concentrations:

$$\ln[(\bar{V}_{\max,i}-V_i)/\bar{V}_{\max,i}] = -k_{o,i}t \tag{5}$$

$\bar{V}_{\max,i}$ values have been evaluated from a set of tests carried out under very high temperature conditions and concluded after very long reaction times, viz. only for those gases whose production continued with time even after 60 min pyrolysis. On the contrary, the maximum values of the experimental curves have been chosen as $\bar{V}_{\max,i}$ for those gases whose production volumes reached maximum values before decreasing (CH_4 and CO_2).

Equation (5) has been used to assess the values of $k_{o,i}$ for the different gases from the slopes of the resulting straight lines.

The specific rate constant $k_{o,i}$ can be related to the thermodynamic temperature (T) by the Arrhenius equation:

$$k_{o,i} = A_i \exp(-E_{act,i}/RT) \tag{6}$$

where A_i is the Arrhenius pre-exponential factor and $E_{act,i}$ the Arrhenius or empirical activation energy, respectively.

The values of $-\ln k_{o,i}$, calculated for each gaseous product at different temperatures, can be plotted versus $1/T$ according to eq. (6); the Arrhenius pre-exponential factor and the activation energy have been calculated from the intercept with the ordinate axis and the slope of the resulting straight line. The values of the activation enthalpy ($\Delta H_{act,i}$), entropy ($\Delta S_{act,i}$) and free energy ($\Delta G_{act,i}$), assuming ideal gas law behaviour, have then been calculated for the supposed first-order reactions through the simultaneous equations [14]:

$$\Delta H_{act,i} = E_{act,i} - RT \tag{7}$$

$$k_{o,i} = (kT/h)\exp(\Delta S_{act,i}/R)\exp(-\Delta H_{act,i}/RT) \tag{8}$$

$$\Delta G_{act,i} = \Delta H_{act,i} - T\Delta S_{act,i} \tag{9}$$

where k and h are Boltzmann's and Planck's constants, respectively.

In order to get some information on the prevailing mechanisms involved in RDF pyrolysis, a reference temperature of 700 °C has been assumed to compare the thermodynamic properties of different functional groups contained in the raw material likely responsible for the production of each gaseous product.

4.2. Model application

The pyrolysis yield, expressed as the ratio between the volumes of gas produced at a given time (V_i) and that related to the total productions ($V_{\max,i}$), has been plotted in Fig. 4 versus the reaction time for the different gaseous products. Owing to the great number of data collected, only those related to

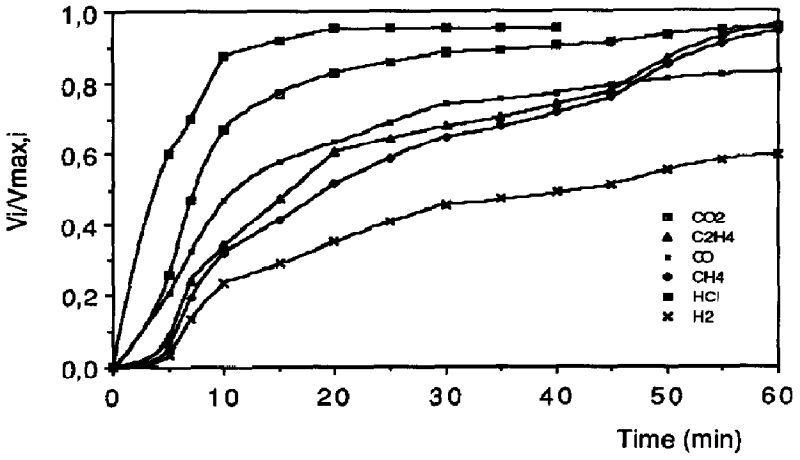

Fig. 4. Yields of gas productions during RDF pyrolysis at 700 °C.

a reference temperature of 700 °C have been plotted, while the complete set of data has been previously reported [15].

A comparison among the starting slopes of the curves in Fig. 4, with reference to the first minutes of pyrolysis, shows that the different products develop with decreasing rates, according to the order:

$$HCl > CO_2 > CO > C_2H_4 > CH_4 > H_2$$

Only the cumulative HCl production curve can be fitted well with an equation proportional to $1-\exp(-k_{0,i}t)$, as it is required by first-order kinetics. Also CO and CO_2 behave as "prompt gases", but both accelerate their productions at around 3 min; the other gases only appear after 5 min. These sigmoid trends have been ascribed to non-isothermal conditions in the early stage of pyrolysis rather than to the presence of consecutive reactions or secondary reactions as proposed for cellulose [9].

The problem related to the kinetic and thermodynamic analysis of sigmoid curves in the presence of non-isothermal starting phases has been exhaustively solved for similar materials, by using a mathematical procedure which subtracts the transition time to the total pyrolysis time, when the non-isothermal phase is very short, like in our case, with respect to total pyrolysis time [11].

The specific rate constants $k_{0,i}$ have been calculated, according to the above described graphic procedure, by plotting $\ln[(\bar{V}_{\max,i}-V_i)/\bar{V}_{\max,i}]$ versus the reaction time. As required by this standard procedure, only the initial production data have to be considered in the present kinetic approach, that is long before achieving the threshold maximum values of the production yields. As an example, Fig. 5 shows the application of this procedure to hydrogen production, which diverges from the first-order equation much more than the other

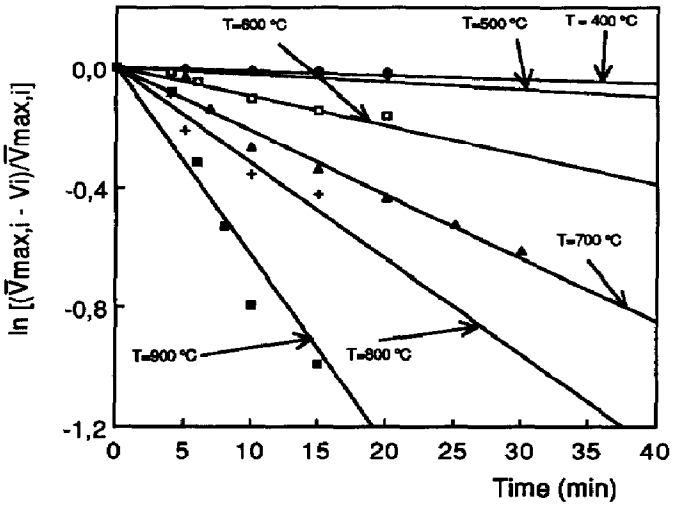

Fig. 5. Graphical evaluation of $k_{0,i}$ for the production of hydrogen during RDF pyrolysis.

TABLE 3

Specific rate constants $k_{0,i}$ (min^{-1}) calculated for the pyrolytic production of gases at different temperatures

Compound	Temperature (°C)				
	400	500	600	700	800
HCl	0.050	0.080	0.116	0.155	0.196
CO_2	0.007	0.021	0.047	0.089	0.149
CO	0.006	0.016	0.032	0.058	0.092
C_2H_4	0.005	0.013	0.026	0.048	0.078
CH_4	0.007	0.013	0.023	0.034	0.048
H_2	0.001	0.004	0.009	0.019	0.035

gases; nevertheless, even in this extreme case consistent deviations seem to occur only at temperatures higher than 800 °C.

In each case, the curvature at the higher temperature, as previously mentioned, could be ascribed to the starting sigmoid trend of gas production versus time rather than to the occurrence of parallel reactions.

The values of the specific rate constants, calculated under different temperature conditions for all the gaseous products, have been listed in Table 3. Besides the expected general increase of the pyrolysis rate with increasing temperature, the figures of Table 3 confirm the above-mentioned qualitative observations on the relative production rates of the different gases. In fact, a comparison of the specific rate constants of the different products at 700 °C shows that the first chemical bonds to react are those (C–Cl) generating

hydrochloric acid, for which an average specific rate constant of 0.155 min^{-1} has been calculated, whereas those responsible for H_2 formation are certainly the least reactive, having a rate constant value nearly one order of magnitude lower ($k_{o,H_2} = 0.019\ min^{-1}$).

The above presented results are proof of the validity of the assumption previously made that the pyrolytic production of gases can be considered as the macroscopic effect of several simultaneous reactions, which behaves, on the whole, as a single first-order production.

4.3. Thermodynamics

The above observations on the different production rates are in agreement with simple thermodynamic considerations on the energies of formation of those bonds contained in the wastes whose rupture can be related to the productions of all the detected gases. In fact, by considering only HCl and H_2 productions — which exhibit the highest and lowest rates respectively — the C–H bonds are usually stronger ($-E_f = 377$–418 kJ/mol) with respect to C–Cl bonds ($-E_f = 335$–356 kJ/mol), whereas the energies of formation for both H_2 and HCl are considerably higher and nearly the same (-431 to -435 kJ/mol).

For a kinetic approach, on the other hand, one should consider and compare the thermodynamic quantities related to the transition states or, at the most, to the reaction intermediates, if any. For this purpose, the values of $k_{o,i}$ obtained at different temperatures, as described above, have been plotted in Fig. 6 as $-\ln k_{o,i}$ versus $1/T$ for every product in order to calculate the empirical activation energy. From these values, the activation enthalpy, entropy and Gibbs energy have been easily calculated for the formation of each transition state. The values of these thermodynamic quantities calculated at the reference temperature of 700 °C have been summarized in Table 4.

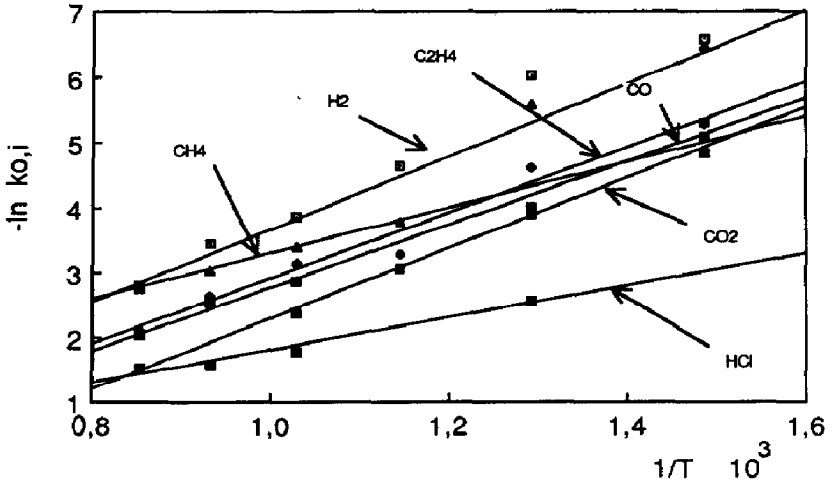

Fig. 6. Arrhenius plots for gas developments during RDF pyrolysis.

TABLE 4

Values of the thermodynamic quantities calculated at 700 °C for the gas productions during RDF pyrolysis

Compound	$E_{act,i}$ (kJ/mol)	$\Delta H_{act,i}$ (kJ/mol)	$\Delta S_{act,i}$ (J/mol K)	$\Delta G_{act,i}$ (kJ/mol)	$k_{o,i}$ (min^{-1})	$V'_{max,i}$ (ml/g)
HCl	20.5	12.4	−283.2	296.1	0.155	1.2
CO_2	45.1	37.0	−262.5	300.6	0.089	42.9
CO	40.8	32.7	−270.5	304.2	0.058	60.0
C_2H_4	41.9	33.8	−270.9	305.5	0.048	3.7
CH_4	29.2	21.1	−286.8	308.3	0.034	21.9
H_2	54.0	45.9	−266.2	313.1	0.019	67.8

Often, in thermodynamic studies, the empirical activation energy ($E_{act,i}$) and the activation enthalpy ($\Delta H_{act,i}$) are numerically similar, so they are used indifferently. In the present case, on the contrary, the activation energies are rather low (compared to RT) with respect to other systems, which means that the percentage difference between $E_{act,i}$ and $\Delta H_{act,i}$ may not be negligible. A confirmation of this is provided when comparing the values for all gaseous products listed in Table 4. However, the absolute values of these two thermodynamic quantities appear to be always an order of magnitude lower than those calculated by several authors for cellulose pyrolysis using different models (from 175.7 to 209.2 kJ/mol) [6, 16, 17]. This suggests that, as expected, the presence of further components in addition to cellulose in this refuse material could completely modify the reaction mechanisms or the physical transport phenomena involved in its pyrolysis.

As regards the strictness of the graphical procedure here presented, it is important to emphasize that thermodynamic extrapolations and subsequent generalizations are more appropriate for ideal homogeneous systems, whereas experimental methods, such as the one under consideration, are the only tools for studying real and/or heterogeneous systems, where any generalization is out of the question.

From the values listed in Table 4 one can observe that the activation entropy reaches a very high negative value ($-295 < \Delta S_{act,i} < -271$ J/mol K) for each of the reactions under consideration.

The observed negative values of $\Delta S_{act,i}$ would be consistent with the formation of transition states having more rigid structures with respect to the reactants; their formation can be supposed in concerted reactions where the formation of a new bond and the rupture of a preexisting bond occur simultaneously. For HCl production, the following mechanisms could all be consistent with the observed values of the activation entropy: (i) concerted β-elimination, (ii) α-elimination with the formation of carbenes in the absence of β-H,

(iii) concerted mechanisms with the formation of free radicals as intermediates and, finally, (iv) radical substitutions. Among these possible mechanisms, the concerted β-elimination and the radical substitutions involve the most rigid structures for the transition states, constituted by a greater number of atoms with respect to the other mechanisms. From the calculated values of $\Delta S_{act,i}$, the most probable mechanism for RDF pyrolysis appears to be the hydrodechlorination via radical substitution, implying the presence of hydrogen atoms linked to the substrate in the transition state. This hypothesis, involving the consumption of only one mole of H_2 per two moles of HCl produced, is consistent with the absence of ethylene among the gaseous products.

Similar concerted mechanisms, like cracking for CH_4 production, have to be supposed for the formation of the other gaseous products; in fact entropy loss variations are about the same as that calculated for HCl.

As regards to the calculated values of the activation free energy, one can observe, as expected, that they are in agreement with the behaviour of $k_{o,i}$, in that $\Delta G_{act,i}$ decreases as the specific rate constant increases. The activation enthalpy, on the contrary, shows a different order of formation rate for the products with respect to $\Delta G_{act,i}$, in that CO_2 and CH_4 are located at different positions on the reactivity and the activation enthalpy scales. This emphasizes, for these concerted reactions, the importance of the activation entropy in calculating the total activation free energy (which is the mere parameter to be considered in kinetic terms). The term $T\Delta S_{act,i}$ is, in the present case, about one order of magnitude higher than $\Delta H_{act,i}$ and thus it absolutely cannot be neglected as often seen with other types of reactions.

The entropic contribution is so important in activation free energy evaluation that $\Delta G_{act,i}$ values substantially higher than those expected from simple qualitative considerations on $E_{act,i}$ have been calculated in this work. This could be the reason for the peculiar slowness of these concerted reactions compared to those of similar thermolyses.

5. Conclusions

Pyrolysis of refuse derived fuel has been studied in this work mainly in terms of product composition and formation rate of each of the gaseous components under different temperature conditions as well as after different reaction times.

Qualitative observation of the production data shows that methane is predominantly formed at temperatures not exceeding 700 °C probably because demethanation prevails over the other cracking reactions, while above this threshold it is degraded into its elements (C and H_2) more rapidly as it is formed. The simultaneous increase of CO and decrease of CO_2 contents in the pyrolysis gas with increasing temperature has been ascribed to Boudouard equilibrium.

The rate of formation of each gaseous product has been calculated from the production data supposing the simultaneous formations of tar, char and gases and that the production of each gaseous product can be roughly described by first-order kinetics. The calculated data have then been used to evaluate, through standard procedures, the values of the main thermodynamic quantities of the reactions leading to the formation of every product ($E_{act,i}$, $\Delta H_{act,i}$, $\Delta G_{act,i}$ and $\Delta S_{act,i}$). Comparison of these amounts gives useful, even if approximate, information on the reaction mechanisms involved in the pyrolysis of refuse derived fuel.

In particular, concerted hydrodechlorination appears to be the most likely mechanism for HCl formation and, in general, similar concerted mechanisms could reasonably be proposed also for the formation of the other gaseous products, as suggested by the high negative values calculated for the activation entropy.

6. Notation

A	Arrhenius pre-exponential factor (min^{-1})
c	concentration of the raw material referring to the only fraction actually convertible into gaseous products (mol/m^3)
E_{act}	Arrhenius activation energy (kJ/mol)
E_f	energy of formation (kJ/mol)
ΔG_{act}	activation free energy (kJ/mol)
ΔH_{act}	activation enthalpy (kJ/mol)
h	Planck's constant (J min)
k	Boltzmann's constant (J/K)
k_o	specific rate constant (min^{-1})
P	concentration of gaseous products (mol/m^3)
R	gas constant (J/mol K)
ΔS_{act}	activation entropy (J/mol K)
t	reaction time (min)
T	temperature (K or °C)
V, $\bar{V}$	volume of produced gases (ml)
V'	specific volume of produced gases (ml/g RDF)

Greek symbols

α	conversion yield

Subscripts

max	maximum threshold values
o	starting values
i	values referred to each gaseous product

References

1 A.G. Buekens and J.G. Schoeters, European experience in the pyrolysis and gasification of solid wastes, Conservation and Recycling, 9 (1986) 253–269.
2 R.K. Agrawal, Kinetics of reactions involved in pyrolysis of cellulose. I. The three reaction model, Can. J. Chem. Eng., 66 (1988) 403–412.
3 R.K. Agrawal, Kinetics of reactions involved in pyrolysis of cellulose. II. The modified Kilzer–Broido model, Can. J. Chem. Eng., 66 (1988) 413–418.
4 C.A. Koufopanos, G. Maschio and A. Lucchesi, Kinetic modelling of the pyrolysis of biomass and biomass components, Can. J. Chem. Eng., 67 (1989) 75–84.
5 F. Thurner and U. Mann, Kinetic investigation of wood pyrolysis, Ind. Eng. Chem. Process Des. Dev., 20 (1981) 482–488.
6 A.E. Lipska and W.J. Parker, Kinetics of pyrolysis of cellulose in the temperature range 250–300 °C, J. Appl. Polym. Sci., 10 (1966) 1439–1453.
7 F. Shafizadeh, Introduction to pyrolysis of biomass, J. Anal. Appl. Pyrolysis, 3 (1982) 283–305.
8 D.S. Scott and J. Piskorz, The continuous flash pyrolysis of biomass, Can. J. Chem. Eng., 62 (1984) 404–412.
9 C.A. Koufopanos, N. Papayannakos, G. Maschio and A. Lucchesi, Modelling of the pyrolysis of biomass particles. Studies on kinetics, thermal and heat transfer effects, Can. J. Chem. Eng., 69 (1991) 907–915.
10 M. Rovatti, M. Bisi, E. Palazzi and G. Ferraiolo, Pirolisi di combustibile derivato dai rifiuti solidi urbani (MRDF), Acqua-Aria (Milan), (2) (1992) 127–133 (with English abstract).
11 J.M. Bouvier, F. Charbel and M. Gelus, Gas–solid pyrolysis of tire wastes. Kinetics and materials balances of batch pyrolysis of used tires, Resour. Conserv., 15 (1987) 205–214.
12 UNICHIM, Misure alle emissioni-flussi convogliati: determinazione del cloro e dell' acido cloridrico, metodo colorimetrico (EM/12), UNICHIM, Milano, 1983, M.U. no. 607, pp. 1–16 (in Italian).
13 E.L. Queen and C.L. Jones, Carbon Dioxide, Reinhold, New York, 1936, pp. 132–133.
14 A.A. Frost and R.G. Pearson, Kinetics and Mechanism, 2nd edn., Wiley, New York, 1963, pp. 98–100.
15 M. Bisi and M. Ferro, Pirolisi dei RSU, Thesis, Faculty of Engineering, Genoa University, Genoa, 1989 (in Italian).
16 P.K. Chatterjee, Chain reaction mechanism of cellulose pyrolysis, J. Appl. Polym. Sci., 12 (1968) 1859–1864.
17 A.F. Roberts, Kinetics of cellulose pyrolysis, J. Appl. Polym. Sci., 14 (1970) 244–247.